Modeling atmospheric sulfate oxidation chemistry via the oxygen isotope anomaly using the Community Multiscale Air Quality Model (CMAQ)

Huan Fang[1], Wendell Walters[1]

[1]Department of Chemistry and Biochemistry, University of South Carolina, SC, 631 Sumter Street Columbia, SC 29208, United States

Correspondence to: Wendell Walters (wendellw@mailbox.sc.edu)

Abstract. Atmospheric sulfate formation influences climate and air quality, yet its chemical pathways remain difficult to constrain. This study utilizes the oxygen isotope anomaly ($\Delta^{17}O$) of sulfate aerosol (ASO_4) as a tracer to distinguish formation processes. This work presents a simulation of $\Delta^{17}O(ASO_4)$ within the contiguous United States, conducted over full annual cycles, which enables the quantification of seasonal and spatial patterns of sulfate oxidation pathways and their response to major emission reductions, for the first time at this scale and temporal coverage. In 2019, $\Delta^{17}O(ASO_4)$ values were predicted to be below 1‰ in the Gulf Coast, indicating acidic, ASO_4-rich conditions dominated by $S(IV) + H_2O_2$ oxidation, while values above 2‰ in the West suggested less acidic conditions, leading to enhanced ASO_4 production via $S(IV) + O_3$ oxidation. Peak $\Delta^{17}O(ASO_4)$ values of ~4.5‰ in April across the Western US reflected O_3-driven ASO_4 formation during high ammonia (NH_3) emissions from fertilization. Between 2006 and 2019, mean $\Delta^{17}O(ASO_4)$ was predicted to increase by up to 2‰, driven by declining sulfur dioxide (SO_2) emissions from regulatory measures. Model comparisons with historical measurements show reasonable agreement in the acidic southeastern US (RMSE = 0.20‰, Baton Rouge, LA). However, the model overpredicts $\Delta^{17}O(ASO_4)$ in the Western US with RMSE values of 0.36‰ (La Jolla, CA) and 1.9‰ (White Mountain Research Center, CA). This overestimation suggests an excessive model response to aqueous $S(IV) + O_3$ reactions. These findings underscore the diagnostic potential of $\Delta^{17}O(ASO_4)$ for assessing sulfate formation mechanisms and pinpointing shortcomings in chemical transport models. However, $\Delta^{17}O(ASO_4)$ observations across the United States remain exceedingly limited, with most available data dating back to the late 1990s and early 2000s, highlighting the need for renewed measurement efforts.

1 Introduction

Atmospheric sulfate (SO_4^{2-}) plays a critical role in climate and air quality. As a major component of aerosols, SO_4^{2-} influences aerosol pH, atmospheric chemistry, and precipitation acidity (Calvo et al., 2013; Weber et al., 2016). SO_4^{2-} aerosols (ASO_4) significantly contribute to radiative forcing by scattering sunlight and serving as cloud condensation nuclei, which impacts cloud properties and the Earth's radiation balance (Lohmann & Feichter, 1997; Jones et al., 1994; Kaufman & Tanré, 1994).

The anthropogenic influence on the ASO_4 budget, primarily from fossil fuel combustion, has been widely documented, contributing to regional and global climate effects (Langner et al., 1992; Smith et al., 2011). The presence of ASO_4 alters cloud albedo and lifetime, affecting regional and global climate patterns through indirect radiative forcing (Jones et al., 1994; Haywood & Boucher, 2000). Additionally, the health impacts of ASO_4-containing particles underscore their importance in air quality management (Reiss et al., 2007). The formation of ASO_4 is influenced by complex interactions with secondary organic aerosols (SOA) and other atmospheric components. Emerging research highlights the significant role of highly oxygenated organic molecules (HOMs) in enhancing ASO_4 formation under humid conditions (Hallquist et al., 2009; Bianchi et al., 2019). These interactions highlight the complex connections between ASO_4, atmospheric chemistry, and climate dynamics. Despite a 70% reduction in ASO_4 concentrations over the past 15 years, aerosol acidity has remained high, primarily due to the buffering effect of ammonia partitioning between the gas and particle phases (Weber et al., 2016). This persistent acidity impacts both air quality and health, as it enhances the solubility of harmful metals and promotes acid-catalyzed chemical reactions in the atmosphere.

Despite their significance, atmospheric chemistry models often face significant challenges in accurately reproducing ASO_4 concentrations, potentially due to uncertainties surrounding ASO_4 formation mechanisms (Harris et al., 2013; Li et al., 2020; Vannucci et al., 2024). ASO_4 can originate from both primary emissions and secondary formation. Primary sources include natural emissions, such as sea salt, volcanic eruptions, and soil dust (Alexander et al., 2005; Arimoto et al., 2001; Savarino et al., 2003), as well as anthropogenic emissions from fossil fuel combustion (Langner et al., 1992; Smith et al., 2011; Solfen et al., 2011). Secondary ASO_4 formation involves complex oxidation processes that occur in both the gas phase and the aqueous phase. In the gas phase, sulfur dioxide (SO_2) is oxidized by hydroxyl radicals ($\cdot OH$), producing sulfuric acid (H_2SO_4). This sulfuric acid can either condense to form new particles or add mass to existing aerosols. The rate of this process is highly dependent on environmental conditions such as temperature and pH, which introduces significant uncertainties in predicting ASO_4 concentrations (Seigneur & Saxena, 1988). For instance, Vannucci et al. (2024) demonstrated that temperature plays a crucial role in modulating ASO_4 aerosol concentrations, particularly during summertime pollution episodes, where aerosol composition and temperature sensitivity can significantly impact model accuracy. Aqueous-phase ASO_4 formation occurs when dissolved sulfur species ($S(IV) = SO_2 \cdot H_2O + HSO_3^- + SO_3^{2-}$) are oxidized by molecules including ozone (O_3), hydrogen peroxide (H_2O_2), and oxygen, catalyzed by transition metal ions (TMI) (e.g., Fe^{3+} and Mn^{2+}). The role of other oxidants, such as hypohalous acids (HOX, X = Cl and Br), is increasingly recognized, particularly in marine boundary layers (Chen et al., 2016; Ishino et al., 2017). Chen et al. (2016) highlighted the significant contribution of HOX in ASO_4 formation in the remote marine boundary layer, estimating that 33-50% of ASO_4 is produced via this pathway. This suggests that HOX may play a larger role in ASO_4 formation than previously recognized. Additionally, aqueous oxidation of SO_2 by nitrogen dioxide (NO_2) has also been proposed as a potential pathway, particularly under polluted and low-oxidant wintertime conditions (Sarwar et al., 2013). Although generally less important than H_2O_2 and O_3 oxidation, this pathway may contribute to ASO_4 formation in specific environments and conditions.

Deleted: , with emerging

Deleted: highlighting

Deleted: sulfate

Deleted: largely driven by

Deleted: eruption

Deleted: , occurring

Deleted: (

Deleted: critical

Deleted: sulfate

Deleted: strongly influence

Moved (insertion) [1]

Moved (insertion) [2]

Sensitivity analyses have shown that the rate of aqueous-phase ASO_4 formation is particularly influenced by pH, oxidant availability, and environmental conditions, further complicating ASO_4 modeling (Pandis & Seinfeld, 1989). Harris et al. (2013) showed that TMI-catalyzed oxidation can dominate under specific conditions, particularly in the presence of coarse dust

100 particles, significantly altering ASO_4 formation rates in cloud droplets. Similarly, Li et al. (2020) highlighted the critical role of TMI-driven SO_2 oxidation during haze episodes, where such pathways can account for up to 50% of ASO_4 production under polluted conditions. Heterogeneous reactions on aerosol surfaces may also play a critical role in ASO_4 formation (Harris et al., 2013). These surface reactions involve the interaction of gaseous sulfur species with aerosols, significantly influencing ASO_4 formation and elevating the complexity of predicting ASO_4 concentrations. Meidan et al. (2019) emphasized the importance

105 of Criegee intermediates (CIs) in ASO_4 formation, particularly in nocturnal power plant plumes, where SO_2 is oxidized under conditions with minimal photochemical activity. This study revealed that CIs could account for a significant portion of ASO_4 production in the absence of sunlight. Additionally, Liu et al. (2019) examined the role of stabilized Criegee intermediates (sCIs) in ASO_4 formation in the Beijing-Tianjin-Hebei region, showing that under certain atmospheric conditions, sCI-driven SO_2 oxidation can contribute substantially to secondary ASO_4 production, adding another layer of complexity to ASO_4

110 formation models. These interactions highlight the challenges in modeling ASO_4 concentrations, as heterogeneous reactions, TMIs, and Criegee intermediates all contribute to the uncertainty in atmospheric ASO_4 predictions.

The use of oxygen isotope mass-independent fractionation ($\Delta^{17}O = \delta^{17}O - 0.52 \times \delta^{18}O$) has emerged as a promising tool to explore atmospheric ASO_4 formation pathways (Alexander et al., 2004; Barkan & Luz, 2003; Kaiser et al., 2004; Michalski et

115 al., 2003; Morin et al., 2007; Savarino et al., 2007; Walters et al., 2019; Weston, 2006). This isotopic indicator is crucial for tracking ASO_4 formation, providing a refined tool for model evaluation and prediction. This is because $\Delta^{17}O$ has distinct values associated with different oxidation processes, making it a powerful tool in understanding ASO_4 production mechanisms. The dominant source of $\Delta^{17}O$ in the lower atmosphere derives from O_3 formation. The average $\Delta^{17}O(O_3)$ near the surface is approximately 26‰ (Vicars & Savarino, 2014). This contrasts with other tropospheric oxidants, which have $\Delta^{17}O$ values near

120 0‰. Hydrogen peroxide (H_2O_2) has a $\Delta^{17}O$ value of about 1.6‰ due to the influence of O_3 involved in H_2O_2 formation (Savarino & Thiemens, 1999). Laboratory studies have shown that oxidants will proportionally transfer their $\Delta^{17}O$ values into the ASO_4 product. Table 1 summarizes the $\Delta^{17}O$ ranges associated with major tropospheric ASO_4 production pathways based on oxygen isotopic mass balance (Alexander et al., 2005; Alexander et al., 2009; Ishino et al., 2017; Savarino et al., 2000; Walters et al., 2019). The gas-phase oxidation of SO_2 by OH and metal-catalyzed O_2 oxidation yields $\Delta^{17}O(ASO_4)$ values near

125 0‰, indicating a negligible transfer of the $\Delta^{17}O$ signature. Similarly, aqueous-phase oxidation of SO_2 by hypohalous acids (HOX) results in $\Delta^{17}O(ASO_4)$ values around 0‰. In contrast, aqueous-phase oxidation involving H_2O_2 and O_3 exhibits significantly higher $\Delta^{17}O$ values. H_2O_2 oxidation produces $\Delta^{17}O(ASO_4)$ values around 0.8‰, while O_3 oxidation results in $\Delta^{17}O(ASO_4)$ values of about 6.5‰. These distinctions enable the ability to track ASO_4 formation.

Previous studies have utilized $\Delta^{17}O(ASO_4)$ observations to evaluate the impact of anthropogenic emissions on ASO_4 production routes. In polluted regions, anthropogenic emissions of metals such as Fe^{3+} and Mn^{2+} enhance O_2-catalyzed ASO_4 formation, particularly in the Northern Hemisphere during winter. This metal-catalyzed ASO_4 formation can suppress ASO_4 production via O_3 and H_2O_2 pathways, impacting $\Delta^{17}O(ASO_4)$ values and complicating model predictions (Savarino et al., 2000). Furthermore, ship emissions, which have been underrepresented in atmospheric models, significantly contribute to ASO_4 source in marine environments. Triple-oxygen isotope measurements suggest these emissions play a larger role in ASO_4 production than previously recognized, with implications for air quality and climate modeling (Dominguez et al., 2008).

To fully utilize the diagnostic potential of $\Delta^{17}O(ASO_4)$, a comprehensive model framework is essential for interpreting ASO_4 formation. Previous models, such as GEOS-Chem, have incorporated $\Delta^{17}O$ tracking to investigate ASO_4 formation pathways, highlighting the growing importance of metal-catalyzed O_2 oxidation in polluted regions, which surpasses the traditional O_3 and H_2O_2 pathways (Sofen et al., 2011). Despite rising tropospheric O_3 levels since preindustrial times, $\Delta^{17}O(ASO_4)$ values in the Arctic have declined due to enhanced metal-catalyzed ASO_4 formation. Recent studies have applied $\Delta^{17}O$ of ASO_4 in chemical transport models to explore long-term changes and regional processes, including GEOS-Chem simulations coupled with ice core observations (Hattori et al., 2021; Peng et al., 2023) and CMAQ applications in East Asia (Itahashi et al., 2022; Lin et al., 2025). These works highlight the diagnostic potential of $\Delta^{17}O$ across diverse regions and timescales. Building upon these advances, our study presents the first CMAQ simulations of $\Delta^{17}O(ASO_4)$ within the contiguous United States over full annual cycles for 2006 and 2019, allowing for the assessment of seasonal and spatial patterns of ASO_4 oxidation pathways in response to emission reductions.

In this work, $\Delta^{17}O$ tracking has now been incorporated into the Community Multiscale Air Quality Model (CMAQ), a 3-D atmospheric chemistry transport model. CMAQ offers high spatial and temporal resolution, which is critical for studying ASO_4 formation pathways and for validating model predictions through observational testing (Appel et al., 2021). This study aims to refine ASO_4 formation modeling by integrating $\Delta^{17}O$ tracking into CMAQ, thus improving predictions of ASO_4 dynamics and reducing uncertainties in atmospheric chemistry models, with a focus on the contiguous US. The spatiotemporal $\Delta^{17}O$ values predicted by CMAQ will help validate model predictions and advance our understanding of atmospheric ASO_4 chemistry and its connection to air quality and deposition. Establishing reference $\Delta^{17}O$ values across the contiguous United States (CONUS) is a key outcome of this study, as it lays the groundwork for future research, enhances air quality and deposition-related studies, and contributes to improved air quality management strategies by providing a more accurate representation of ASO_4 formation across different regions.

Table 1: Major ASO_4 formation pathways and their associated $\Delta^{17}O$ signatures. The pathways that are included in the CMAQ model using the cb6r5-ae7-aq mechanism are indicated.

Pathway	Reaction	$\Delta^{17}O$ (‰)	Notes	Included in CMAQ (cb6r5-ae7)

Gas-Phase	$SO_2 + \cdot OH \rightarrow SO_4^{2-} + HO_2$	~0	Dominant in photochemically active regions; negligible $\Delta^{17}O$ signature	Yes
Gas-Phase	$SO_2 + sCI$ (Stabilized Criegee Intermediates) $\rightarrow SO_4^{2-}$	~0	Can enhance secondary ASO_4 formation in regions influenced by biogenic VOC emissions; negligible $\Delta^{17}O$ signature	NO
Aqueous-Phase	$HSO_3^- + H_2O_2 \rightarrow SO_4^{2-} + H_2O$	0.8	Lower $\Delta^{17}O$ value, dominant under humid/cloudy conditions.	Yes
Aqueous-Phase	$SO_3^{2-} + O_3 \rightarrow SO_4^{2-} + O_2$	6.5	Higher $\Delta^{17}O$ value, significant for cloud chemistry.	Yes
Aqueous-Phase	$SO_3^{2-} + O_2$ (TMI = Transition Metal Ions, e.g., Fe^{3+} and Mn^{2+}) $\rightarrow SO_4^{2-}$	~0	Important in metal-rich aerosols; negligible $\Delta^{17}O$ signature	Yes
Aqueous-Phase	$SO_3^{2-} + NO_2 \rightarrow SO_4^2 + NO$	~0	Relevant under polluted and low-oxidant wintertime conditions; negligible $\Delta^{17}O$ signature	No
Aqueous-Phase	$SO_3^{2-} + HOX$ (X = Br, Cl) $\rightarrow SO_4^{2-}$	~0	Dominant in marine environments with halogen chemistry; negligible $\Delta^{17}O$ signature	No
Heterogeneous	SO_2 (surface) + Organic peroxides $\rightarrow SO_4^{2-}$	~0	Significant role in submicron aerosol ASO_4 formation; negligible $\Delta^{17}O$ signature.	No
Heterogeneous	SO_2 (surface) + H_2O_2 or O_3 on aerosols $\rightarrow SO_4^{2-}$	0.8 - 6.5	Highly variable; depends on aerosol composition and environmental conditions.	No

425

2 Methods

2.1 Model Description and EQUATES 2019 Dataset

This study utilizes the CMAQ (Community Multiscale Air Quality) version 5.4 model to simulate ASO_4 formation and its $\Delta^{17}O$ values across the contiguous United States (CONUS). The CMAQ model is configured with the cb6r5_ae7_aq chemical mechanism, which stands for Carbon Bond 6 revision 5, with aerosol 7 for standard cloud chemistry (Yarwood et al., 2010). This mechanism encompasses both gas-phase and aqueous-phase oxidation processes of SO_2, which are essential for accurately modeling ASO_4 formation. Specifically, it involves the oxidation of SO_2 by ·OH in the gas phase and by H_2O_2 and O_3 in cloud droplets and aqueous environments. Cloud water pH in CMAQ is calculated dynamically within the default cloud chemistry module, which is based on the work of Walcek and Taylor (1986) and assumes instantaneous equilibrium among gas, aqueous, and ionic species. The pH is determined by the charge balance between dissolved acidic and basic ions. As S(IV) is oxidized to S(VI) and additional species are scavenged from interstitial aerosols, the pH evolves dynamically throughout cloud processing. The resulting pH fields respond to emissions and meteorological variability, directly governing the relative importance of the H_2O_2 and O_3 oxidation pathways for aqueous S(IV) oxidation. Previous evaluations have demonstrated that CMAQ accurately reproduces observed cloud droplet acidity, with differences generally within 0.5 pH units across multiple sites in the United States (Pye et al., 2020). The model's ability to capture these complex interactions facilitates a detailed assessment of ASO_4 dynamics under various atmospheric conditions (Appel et al., 2021).

The CMAQ simulations are based on the EQUATES (EPA's Air Quality Time Series Project) dataset, which provides a comprehensive and high-resolution emissions inventory derived from the 2017 National Emissions Inventory (NEI) (Benish et al., 2022; Foley et al., 2023). This dataset spans over two decades and provides detailed information on both natural and anthropogenic emissions, including those from industrial sources, vehicular traffic, power plants, and wildfires. It also accounts for seasonal and regional variations in emissions, enhancing the model's accuracy. The EQUATES 2019 dataset supplies critical inputs for CMAQ simulations, including emissions data, meteorological variables, as well as boundary and initial conditions, capturing pollutant variability across different seasons and regions.

Meteorological inputs for the CMAQ simulations were integrated from the Weather Research and Forecasting (WRF) model version 4.1.1. This integration provides detailed representations of temperature, wind speed, relative humidity, cloud cover, and precipitation rates. These meteorological factors influence cloud formation, pollutant dispersion, and oxidation processes. Boundary and initial conditions for the CMAQ model were sourced from EQUATES to ensure accurate representation of pollutant inflows and outflows at the edges of the modeling domain. The initial conditions were established through a spin-up period starting on December 15, 2018, providing accurate starting concentrations for the 2019 simulation period. The CMAQ simulations were conducted at a resolution of 12 × 12 km over the CONUS domain using the Hyperion high-performance

computing cluster at the University of South Carolina. This advanced computing infrastructure enabled the processing of large datasets and the execution of complex simulations necessary for this study.

2.2 Implementation of the Sulfur Tracking Mechanism (STM)

The Sulfur Tracking Mechanism (STM), utilized in the CMAQ model, provides a detailed analysis of ASO_4 formation pathways in the atmosphere (Appel et al., 2021). It distinguishes between various aqueous-phase and gas-phase formation processes and assesses contributions from emissions, initial conditions, and boundary conditions, offering valuable insights into the roles of these factors in overall ASO_4 production (Table 2). The sulfur budget comprises 14 ASO_4 species (AE) and 1 nonreactive ASO_4 species (NR), as documented in the CMAQ repository (https://github.com/USEPA/CMAQ/blob/main/CCTM/src/MECHS/README.md). The STM output includes hourly simulations of the 15 tagged ASO_4 species across the model domain, which were then aggregated into monthly averages to analyze spatial and temporal variations in ASO_4 production. STM allows for an efficient way for the model to distinguish the contributions of different chemical pathways and emission contributions to ASO_4. This approach also enables a seamless calculation of $\Delta^{17}O$ of ASO_4.

A known bookkeeping bug in the STM implementation in CMAQ v5.4 resulted in the systematic underestimation of ASO_4 formed via the gas-phase $SO_2 + OH$ pathway, despite the pathway being chemically active in the model. This issue has been documented by the CMAQ development team (https://github.com/USEPA/CMAQ/wiki/CMAQ-Release-Notes:-Process-Analysis-&-Sulfur-Tracking-Model-(STM)) and has since been corrected in version 5.5. In our study, we fixed the issue by adjusting the call order of STM update routines in the sciproc.F module (matching the v5.5 fix) and ran the simulations using the corrected code. The updated STM diagnostic module used in this work is publicly available for reproducibility at: https://doi.org/10.5281/zenodo.14954960.

Table 2: Overview of the ASO_4 species in the Sulfur Tracking Mechanism (STM) incorporated into CMAQ.

Name	Group	Mode	Pathway
ASO4GASI	AE	Aitken	condensation of gas-phase reaction with OH
ASO4EMISI	AE	Aitken	source emission
ASO4ICBCI	AE	Aitken	initial conditions and boundary conditions
ASO4AQH2O2J	AE	Accumulation	H_2O_2
ASO4AQO3J	AE	Accumulation	O_3
ASO4AQFEMNJ	AE	Accumulation	O_2 catalyzed by Fe^{3+} and Mn^{2+}
ASO4AQMHPJ	AE	Accumulation	methyl hydrogen peroxide (MHP)
ASO4AQPAAJ	AE	Accumulation	peroxyacetic acid (PAA)

ASO4GASJ	AE	Accumulation	condensation of gas-phase reaction with OH
ASO4EMISJ	AE	Accumulation	source emission
ASO4ICBCJ	AE	Accumulation	initial conditions and boundary conditions
ASO4GASK	AE	Coarse	condensation of gas-phase reaction with OH
ASO4EMISK	AE	Coarse	source emission
ASO4ICBCK	AE	Coarse	initial conditions and boundary conditions
SULF_ICBC	NR	N/A	sulfuric acid vapor (SULF) from initial conditions and boundary conditions

2.3 Calculation and Analysis of $\Delta^{17}O(ASO_4)$

495 The fractional contributions of each pathway, obtained from the STM, are used to calculate $\Delta^{17}O(ASO_4)$ across different grid cells.

$$f_i(lat, lon, height, time) = \frac{X_i}{\sum_{i=1}^{n} X_i}$$

(1)

where f_i represents the fractional contribution of pathway i; X_i is the amount of ASO_4 produced by pathway i; and $\sum_{i=1}^{n} X_i$ is

500 the total Aitken mode and accumulation mode ASO_4 produced by all pathways except initial conditions and boundary conditions in each grid cell.

The gas-phase oxidation of SO_2 by •OH radical results in ASO_4 with no significant $\Delta^{17}O$ enrichment (~0‰). ASO_4 formed via aqueous-phase oxidation by O_3 has a $\Delta^{17}O$ value of ~6.5‰, indicating significant cloud chemistry processes. ASO_4 formed

505 via aqueous-phase oxidation by H_2O_2 has a $\Delta^{17}O$ value of ~0.8‰. Metal-catalyzed oxidation of SO_2 by O_2 in metal-rich environments results in a $\Delta^{17}O$ value of ~0‰ and does not exhibit a transfer of mass-independent fractionation signature. Although previous studies reported slightly negative $\Delta^{17}O$ values (-0.1‰; Hattori et al., 2021; Itahashi et al., 2022), this pathway contributes less than 10% to total ASO_4 formation in our simulations, leading to a negligible (<0.01‰) effect on the modeled $\Delta^{17}O(ASO_4)$. Therefore, it is approximated as 0‰ in this study. Heterogeneous reactions, such as those involving

510 organic peroxides on aerosol surfaces, contribute to ASO_4 formation and are expected to have a $\Delta^{17}O$ ~0‰. Although the fractional contributions (f_i) include all ASO_4 formation pathways diagnosed by the Sulfur Tracking Mechanism (STM), only H_2O_2 and O_3 carry non-zero $\Delta^{17}O$ signatures, all other pathways are assigned $\Delta^{17}O \approx 0‰$. Therefore, the $\Delta^{17}O(ASO_4)$ is calculated using the following equation:

$$\Delta^{17}O(ASO_4) = f_{ASO4AQH2O2J} \times 0.8‰ + f_{ASO4AQO3J} \times 6.5‰$$

515

(2)

where ASO4AQH2O2J represents ASO$_4$ formed through the oxidation of SO$_2$ by H$_2$O$_2$; ASO4AQO3J represents ASO$_4$ formed through oxidation by O$_3$; the constants 0.8‰ and 6.5‰ correspond to the characteristic Δ^{17}O values for each pathway.

3 Results and Discussion

3.1 Predicted Fractional ASO$_4$ Formation and Δ^{17}O(ASO$_4$) in the Contiguous US in 2019

ASO$_4$ production in the contiguous United States arises from a combination of primary emissions and secondary formation pathways, the latter being dominated by H$_2$O$_2$- and O$_3$-driven aqueous S(IV) oxidation and gas-phase oxidation of SO$_2$ via •OH (Fig. 1). These secondary reactions occur within cloud water, where SO$_2$ is oxidized by H$_2$O$_2$, O$_3$, and by O$_2$ (catalyzed by TMI). Compared to these dominant pathways, the TMI-catalyzed oxidation and reactions involving organic peroxides, such as methyl hydrogen peroxide (MHP) and peroxyacetic acid (PAA), have a minimal impact on ASO$_4$ production. While primary emissions contribute little overall, they exhibit localized hotspots in certain regions.

The fractional contributions of ASO$_4$ formation pathways demonstrate distinct spatial patterns that align with the predicted Δ^{17}O(ASO$_4$) variability. The H$_2$O$_2$ pathway ($f_{S(IV)+H2O2}$) is the most dominant, accounting for 35.4±14.0% of the ASO$_4$ formation across the domain (Fig. 1). This pathway is particularly influential in the Gulf Coast States, where abundant cloud cover and water vapor, acidic conditions (cloud pH < 6), and high concentrations of H$_2$O$_2$ (Fig. S1, Fig. S2) support the oxidation of S(IV) in cloud droplets. The highest $f_{S(IV)+H2O2}$ in these regions contribute to the low Δ^{17}O(ASO$_4$) values below 1‰, due to the relatively lighter Δ^{17}O(ASO$_4$) resulted from the H$_2$O$_2$ pathway (0.8‰). Gas-phase oxidation of SO$_2$ by •OH (f_{SO2+OH}) contributes to 34.4%±9.5 of the ASO$_4$ production across the domain (Fig. 1), exhibiting clear seasonal variability under photochemically active conditions, with the highest contributions occurring in summer (up to ~75 %) and lowest in winter (< 25 %) (Fig. 5). The O$_3$ pathway ($f_{S(IV)+O3}$) is the third most significant, contributing approximately 18.7±5.2% to the ASO$_4$ formation across the domain (Fig. 1). The highest $f_{S(IV)+O3}$ occurs in the Western States, due to the high O$_3$ concentration and high cloud pH (Fig. S1), which facilitates the aqueous oxidation of S(IV) by O$_3$. With a higher Δ^{17}O(ASO$_4$) value resulting from the S(IV) + O$_3$ pathway of 6.5‰, the higher $f_{S(IV)+O3}$ in these regions results in elevated Δ^{17}O(ASO$_4$) values, typically above 2‰. Minor pathways, such as those involving TMI, MHP, and PAA, contribute 2.3±1.8%, 0.25±0.25%, and 0.17±0.12%, respectively (Fig. 1), to ASO$_4$ formation across the US continuous domain. Primary ASO$_4$ emissions account for 8.7±6.4% of total ASO$_4$ (Fig. 1), with substantial contributions originating from urban and industrial regions. High SO$_2$ emissions from anthropogenic activities in these areas elevate the role of primary ASO$_4$, and their impact on Δ^{17}O(ASO$_4$) is correspondingly notable but limited to these localized hotspots.

Cloud pH is a critical determinant of ASO$_4$ formation pathways and Δ^{17}O(ASO$_4$) values, with lower cloud pH favoring the H$_2$O$_2$ pathway and higher cloud pH supporting the O$_3$ pathway (Seigneur & Saxena, 1988; Fahey & Pandis, 2001). The

concentration of ASO_4 plays a dominant role in lowering cloud pH, primarily due to its origin from sulfuric acid (H_2SO_4). As a strong acid, H_2SO_4 dissociates completely, releasing significant amounts of hydrogen ions (H^+) and causing substantial acidification of cloud water. In regions such as the Northeast, Southeast, and Midwest, relatively high SO_2 emissions result in elevated ASO_4 concentrations, which further favor the dominance of the H_2O_2 oxidation pathway over O_3, thereby sustaining low $\Delta^{17}O(ASO_4)$ values in the Northeast and Southeast (Fig. S1). This is due to the efficient conversion of dissolved S(IV) species to ASO_4, primarily through the aqueous $S(IV)+H_2O_2$ pathway under acidic cloud water. Frequent cloud occurrence and abundant oxidant availability accelerate SO_2 to ASO_4 production. These high ASO_4 levels contribute significantly to lowering cloud pH in these areas, creating an acidic environment (Fig. S1). In contrast, in the Western States, SO_2 emissions and ASO_4 concentrations are comparatively lower (Fig. S1). This results in reduced acidification and a higher cloud pH, as the influence of ASO_4 on the acidity of cloud water is diminished. Ammonium in cloud water (ANH_4), on the other hand, primarily acts as a buffering agent, mitigating the acidity caused by ASO_4 (Fig. S1). NH_3 reacts with H_2SO_4 to form $(NH_4)_2SO_4$ (ammonium sulfate), which reduces the availability of free H^+ and partially neutralizes the acidification caused by ASO_4. However, the neutralizing capacity of ANH_4 is limited. In regions with high ASO_4 concentrations, such as the Northeast and Southeast, the buffering effect of ANH_4 is insufficient to fully counteract the strong acidity introduced by ASO_4. In the Midwest, where NH_3 emissions from agricultural activities, particularly fertilization, are significant, the resulting high concentrations of ANH_4 partially neutralize the acidity from ASO_4 (Fig. S1). This interaction raises cloud pH slightly, preventing extreme acidification (Fig. S1). Nevertheless, even in regions with abundant NH_3 emissions, cloud water pH typically remains acidic because of the dominant influence of ASO_4 and other atmospheric acids.

585

590

595
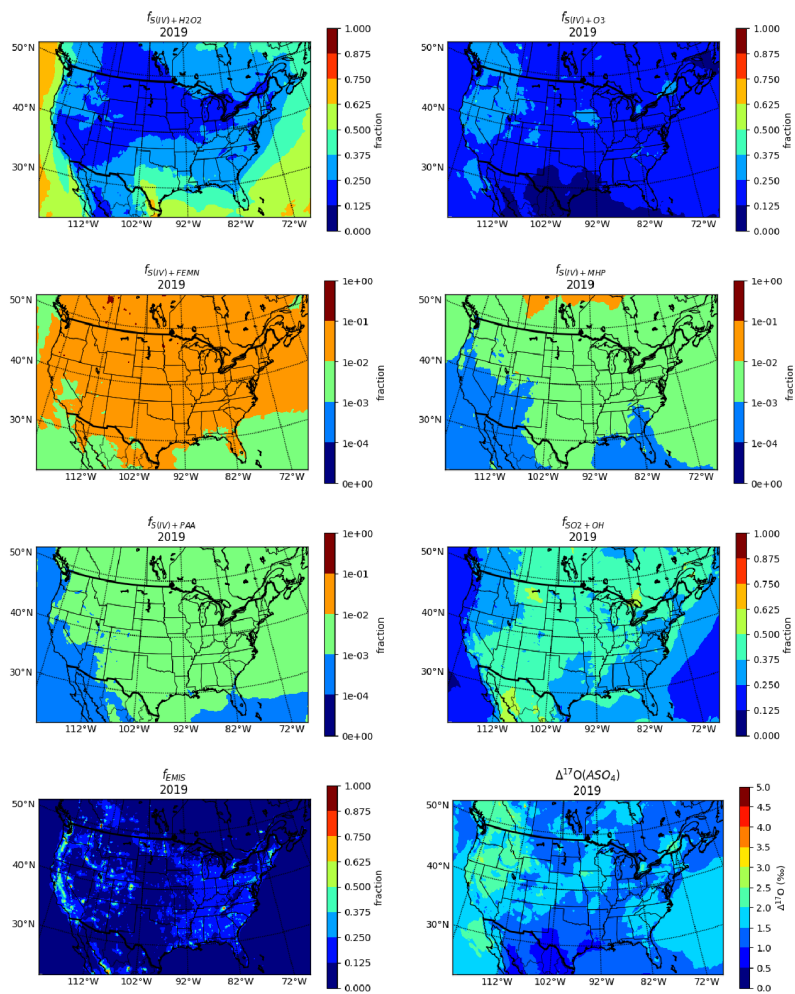
Fig. 1: The annual fractional contribution from each ASO₄ formation pathway, along with $\Delta^{17}O(ASO_4)$ across the contiguous US in the year 2019, based on CMAQ simulation.

3.2 Seasonal Variation in Fractional ASO₄ Formation and Δ¹⁷O(ASO₄) in the Contiguous US in 2019

ASO_4 formation across the contiguous United States exhibits distinct seasonal patterns, shaped by varying contributions from the H_2O_2 and O_3 pathways, as well as shifts in cloud pH and precursor concentrations (Fig. S1). The isotopic composition of ASO_4, represented by $\Delta^{17}O(ASO_4)$, reflects the dominance of specific pathways under different meteorological and chemical conditions. In regions with low cloud pH, the H_2O_2 pathway dominates, resulting in low $\Delta^{17}O$ values (Fig. S1, Fig. 2). Conversely, areas with high cloud pH favor the O_3 pathway, resulting in high $\Delta^{17}O$ values (Fig. S1, Fig. 2). Meanwhile, gas-phase $SO_2 + \cdot OH$ oxidation (Fig. 5) acts as a consistent background process throughout the year. Its near-zero $\Delta^{17}O$ signature moderates the contrast between H_2O_2- and O_3-dominated regimes, with a stronger influence during summer when photochemical activity peaks. Together with seasonal variations in cloud pH, ASO_4, and ANH_4 (Fig. S3, Fig. S4, Fig. S6), this process shapes the overall spatiotemporal pattern of $\Delta^{17}O(ASO_4)$, reflecting the coupled effects of emissions, atmospheric chemistry, and meteorology.

In January, the Western States exhibit the highest $\Delta^{17}O(ASO_4)$ values, exceeding 2‰ (Fig. 2). This is driven by the increased importance of the $S(IV) + O_3$ oxidation pathway (Fig. 3), supported by elevated cloud pH levels resulting from low ASO_4 concentrations (Fig. S3, Fig. S4). Conversely, the Gulf Coast States show the lowest $\Delta^{17}O(ASO_4)$ values, typically below 1‰ (Fig. S1), primarily due to the prevalence of the H_2O_2 pathway (Fig. 4). This pathway dominates under low cloud pH conditions caused by high ASO_4 concentrations and limited ANH_4 levels (Fig. S3, Fig. S4, Fig. S6). In the Midwest, moderate $\Delta^{17}O(ASO_4)$ values are shown, reflecting a balance between pathways. Elevated ANH_4 levels partially neutralize the acidity from high ASO_4 concentrations (Fig. S4, Fig. S6). This neutralization raises cloud pH (Fig. S3), slightly lowering the fractional contribution of the $S(IV) + H_2O_2$ pathway (Fig. 4) and contributing to the intermediate $\Delta^{17}O(ASO_4)$ values. During this period, the $SO_2 + \cdot OH$ pathway remains weak due to limited photochemical activity but provides a modest background effect that slightly reduces the isotopic contrast between H_2O_2- and O_3-dominated regimes.

In April, $\Delta^{17}O$ values increase significantly, particularly in the Western States, rising above 3‰ (Fig. 2). This trend indicates an enhanced influence of the O_3 pathway, supported by elevated cloud pH and increased O_3 levels (Fig. 3, Fig. S3, Fig. S8). In contrast, the Gulf Coast States continue to exhibit low $\Delta^{17}O$ values (<1.5‰) (Fig. 2), as the H_2O_2 pathway remains dominant due to persistently low cloud pH (Fig. 4, Fig. S3). This acidity is driven by high ASO_4 concentrations and low ANH_4 concentrations (Fig. S4, Fig. S6). Meanwhile, in the Midwest, cloud pH begins to rise as increased NH_3 levels, partially neutralizing the acidity from ASO_4 and shifting the balance of ASO_4 formation pathways (Fig. S3, Fig. S4, Fig. S7). The influence of the $SO_2 + \cdot OH$ pathway decreases relative to January (Fig. 5), as O_3 oxidation becomes more dominant, thereby exerting a weaker moderating effect on the isotopic contrast across regions.

In July, $\Delta^{17}O$ values decrease in the Western States as the $f_{S(IV)+H2O2}$ increases compared to April (Fig. 2). This shift is driven by higher water vapor levels and increased cloud cover (Fig. S10), despite the regional consistently high cloud pH (Fig. S3). In the Gulf Coast States, $\Delta^{17}O$ values remain low, below 1.5‰ (Fig. S1), highlighting the continued dominance of the H_2O_2 pathway (Fig. 4) under conditions of abundant water vapor (Fig. S10), frequent cloud cover (Fig. S11), and persistently low cloud pH (Fig. S3). In the Midwest, cloud pH continues to rise from April (Fig. S3), driven by increasing NH_3 concentrations (Fig. S7), which partially neutralize the acidity caused by ASO_4 (Fig. S4). This elevation in cloud pH enhances the activity of the O_3 pathway (Fig. S2), leading to an increase in $\Delta^{17}O$ values compared to April. At the same time, the $SO_2 + \cdot OH$ pathway reaches its maximum importance (Fig. 5) under strong photochemical conditions, offsetting the isotopic enrichment from O_3 oxidation and contributing to the relative decrease in $\Delta^{17}O(ASO_4)$ compared to April.

In October, $\Delta^{17}O$ values in the Western States increase compared to July but remain slightly lower than in April (Fig. 2). This change is attributed to the enhanced $f_{S(IV)+O3}$ (Fig. S2), supported by high cloud pH and low ASO_4 concentrations (Fig. S3, Fig. S4). In the Gulf Coast States, $\Delta^{17}O$ values remain low (Fig. 2), reflecting the continued dominance of the H_2O_2 pathway under acidic conditions sustained by high ASO_4 levels and low ANH_4 concentrations (Fig. S3, Fig. S4, Fig. S6). In the Midwest, decreasing NH_3 levels from July reduce the neutralization of acidity (Fig. S3, Fig. S7), making conditions less favorable for O_3-driven ASO_4 formation (Fig. 3). This results in lower cloud pH (Fig. S3) and diminished $\Delta^{17}O$ values compared to earlier months. As photochemical activity weakens, the relative contribution of the $SO_2 + \cdot OH$ pathway declines (Fig. 5), reducing its moderating effect and allowing O_3-driven isotopic enrichment to strengthen in high-pH regions.

Seasonal variations in ASO_4 formation and $\Delta^{17}O(ASO_4)$ highlight the interplay of chemical drivers and meteorological conditions. The dominance of the H_2O_2 pathway in acidic, ASO_4-rich regions, such as the Gulf Coast States, leads to low $\Delta^{17}O$ values year-round. In contrast, the O_3 pathway prevails in higher pH regions such as the Western States, driving elevated $\Delta^{17}O$ values, particularly in April. The Midwest experiences transitional conditions, where cloud pH and NH_3 concentrations modulate the relative contributions of ASO_4 formation pathways. Alongside these seasonal and spatial contrasts, the gas-phase $SO_2 + \cdot OH$ pathway acts as a persistent, near-zero-$\Delta^{17}O$ background that offsets isotopic enrichment from O_3 oxidation, particularly during summer when photochemical activity peaks. These findings underscore the dynamic nature of ASO_4 chemistry across seasons, emphasizing the importance of emissions, atmospheric composition, and cloud chemistry in shaping regional and seasonal patterns of ASO_4 formation.
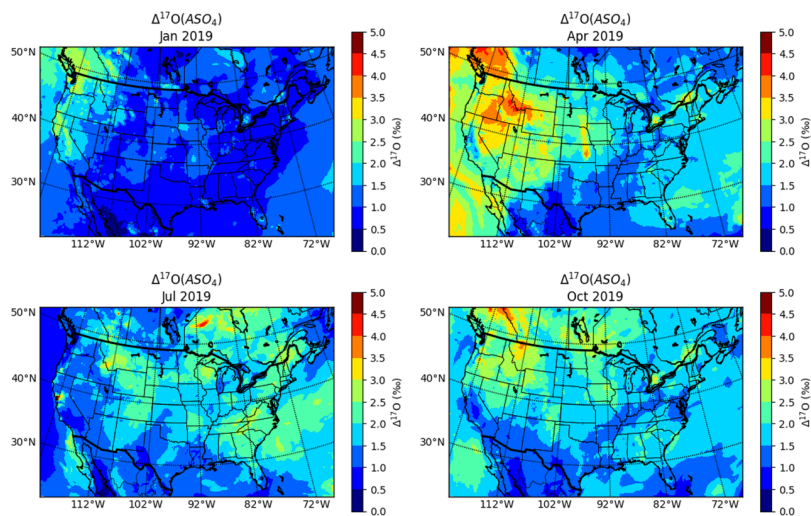
705   **Fig. 2: The** ~~simulated~~ **$\Delta^{17}O(ASO_4)$ values across the** ~~contiguous~~ **US for the year 2019 in each season (winter: Jan, spring:**
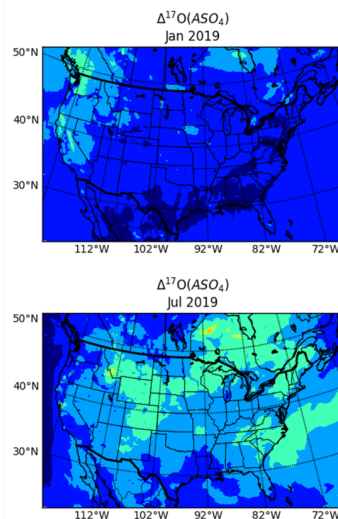
Apr, summer: July, fall: Oct), based on CMAQ simulation.
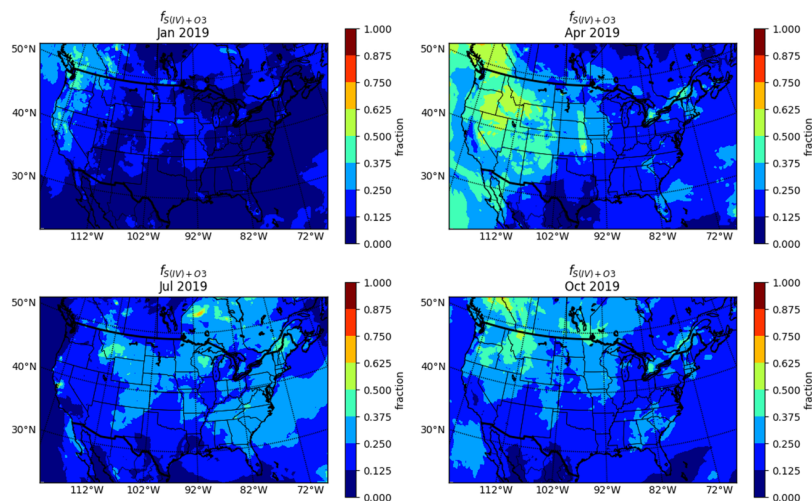
Fig. 3: The fraction of ASO$_4$ formation from S(IV)+O$_3$ pathway across the contiguous US for the year 2019 in each season (winter: Jan, spring: Apr, summer: July, fall: Oct), based on CMAQ simulation.
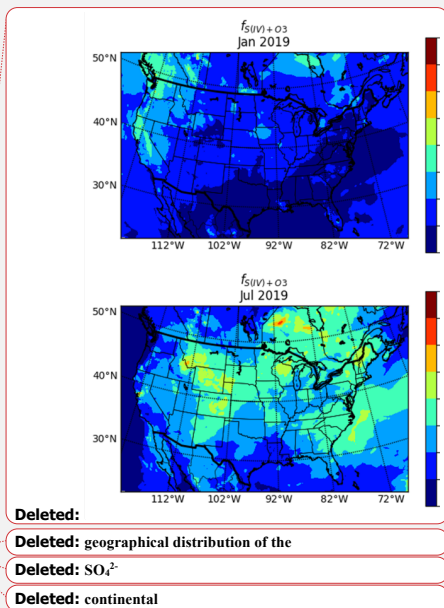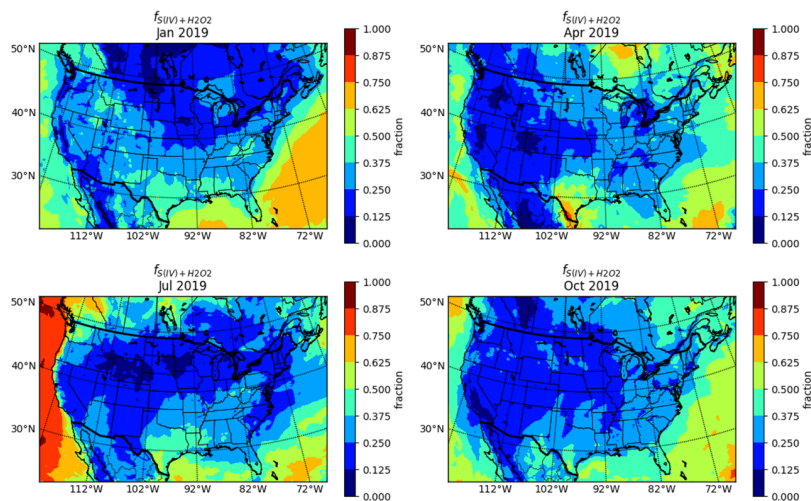
720 **Fig. 4: The fraction of ASO$_4$ formation from S(IV)+H$_2$O$_2$ pathway across the contiguous US for the year 2019 in each season (winter: Jan, spring: Apr, summer: July, fall: Oct), based on CMAQ simulation.**
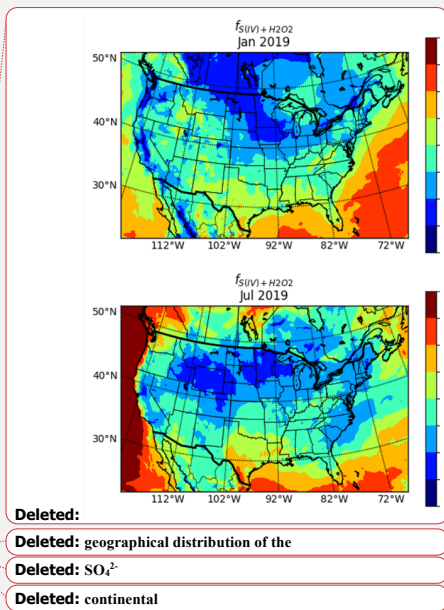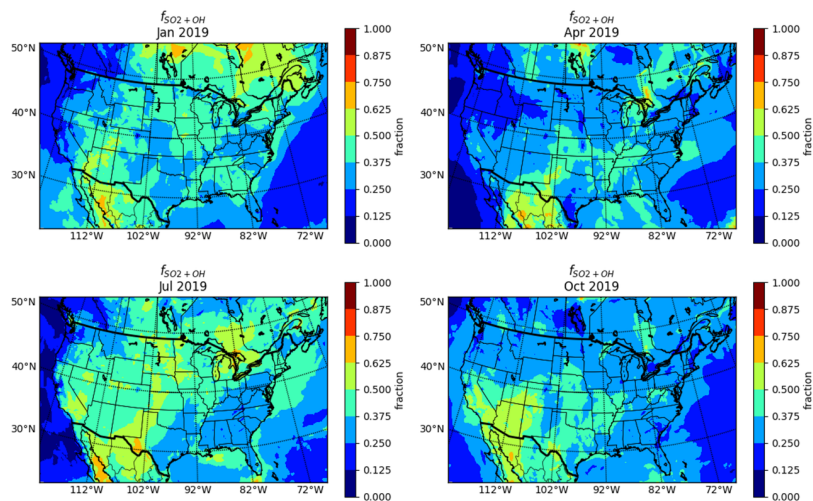
Fig. 5: The fraction of ASO₄ formation from SO₂ + OH pathway across the contiguous US for the year 2019 in each season (winter: Jan, spring: Apr, summer: July, fall: Oct), based on CMAQ simulation.

730
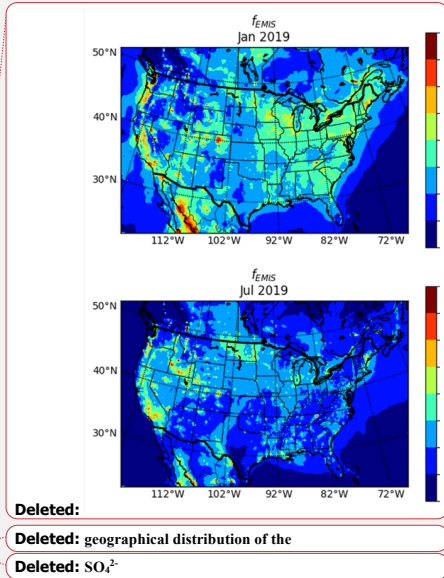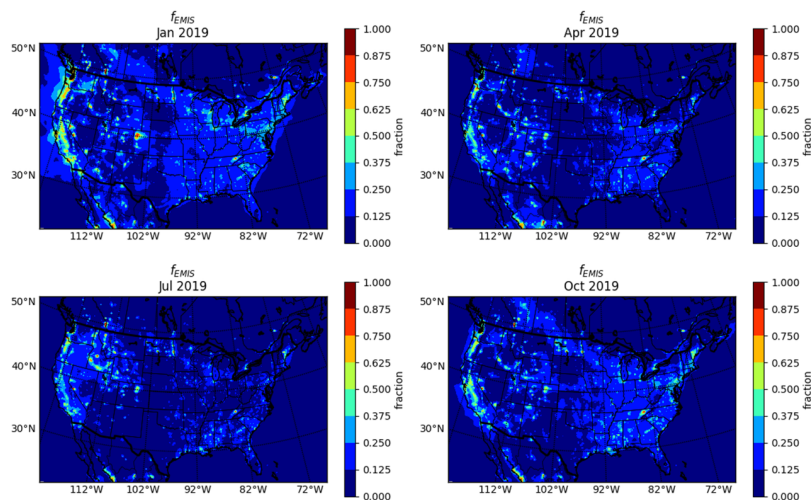
Fig. 6: The fraction of ASO₄ from primary emission across the contiguous US for the year 2019 in each season (winter: Jan, spring: Apr, summer: July, fall: Oct), based on CMAQ simulation.

3.3 Change in Fractional Annual ASO₄ Formation and Δ¹⁷O(ASO₄) from 2006 to 2019

From 2006 to 2019, the annual $\Delta^{17}O(ASO_4)$ values across the contiguous US showed a consistent increase, highlighting the growing importance of the O_3 pathway in ASO₄ formation (Fig. 7). In the central and eastern US, $\Delta^{17}O(ASO_4)$ values increased by up to 2‰ (Fig. 7), primarily driven by significant reductions in SO_2 emissions, largely attributable to regulatory measures such as the Clean Air Act. These reductions led to lower ASO₄ concentrations, which elevated cloud pH and shifted the ASO₄ formation process toward the O_3 pathway (Fig. S12), resulting in ASO₄ with higher $\Delta^{17}O$ values. Conversely, the western US exhibited only modest increases in $\Delta^{17}O(ASO_4)$, typically less than 1‰ (Fig. 7). This is because the region historically favored O_3-dominated ASO₄ formation due to consistently high O_3 and cloud pH levels (Fig. S13), making the impacts of rising cloud pH and reduced SO_2 emissions less obvious. Changes in H_2O_2 concentrations played a significant role in shaping these trends. In the central and eastern US, slight increases in H_2O_2 concentrations continued to support the H_2O_2 pathway, to a limited extent, even as the O_3 pathway became more dominant (Fig. 7, Fig. S12). In contrast, in the western US, H_2O_2 concentrations decreased slightly, resulting in a slight reduction in $f_{S(IV)+H2O2}$ (Fig. 7). A decrease in f_{SO2+OH} across the domain along with the negligible contributions from other pathways caused a relative increase in f_{EMIS} in these regions (Fig. 7). Between 2006 and 2019, the domain-averaged f_{SO2+OH} decreased by 12.5%, primarily due to the enhanced contribution of the O_3 oxidation

pathway ($f_{f_{S(IV)+O_3}}$) and lower SO_2 concentrations under reduced precursor emissions, which together shifted the overall oxidation balance toward aqueous-phase processes. Consistent with these trends, spatial patterns of concentration changes (Fig. S12) show substantial decreases in SO_2 and ASO_4, particularly in the eastern US, while NH_3 and ANH_4 increased, leading to higher cloud pH and favoring O_3 oxidation. Meanwhile, primary ASO_4 emissions, which do not carry a mass-independent

770 signature and exhibit $\Delta^{17}O$ values close to 0‰, directly added to ASO_4 levels and tempered changes in $\Delta^{17}O(ASO_4)$ values (Fig. 7). This dynamic explains why the increases in $\Delta^{17}O(ASO_4)$ values from 2006 to 2019 were smaller in the western US compared to the central and eastern regions.
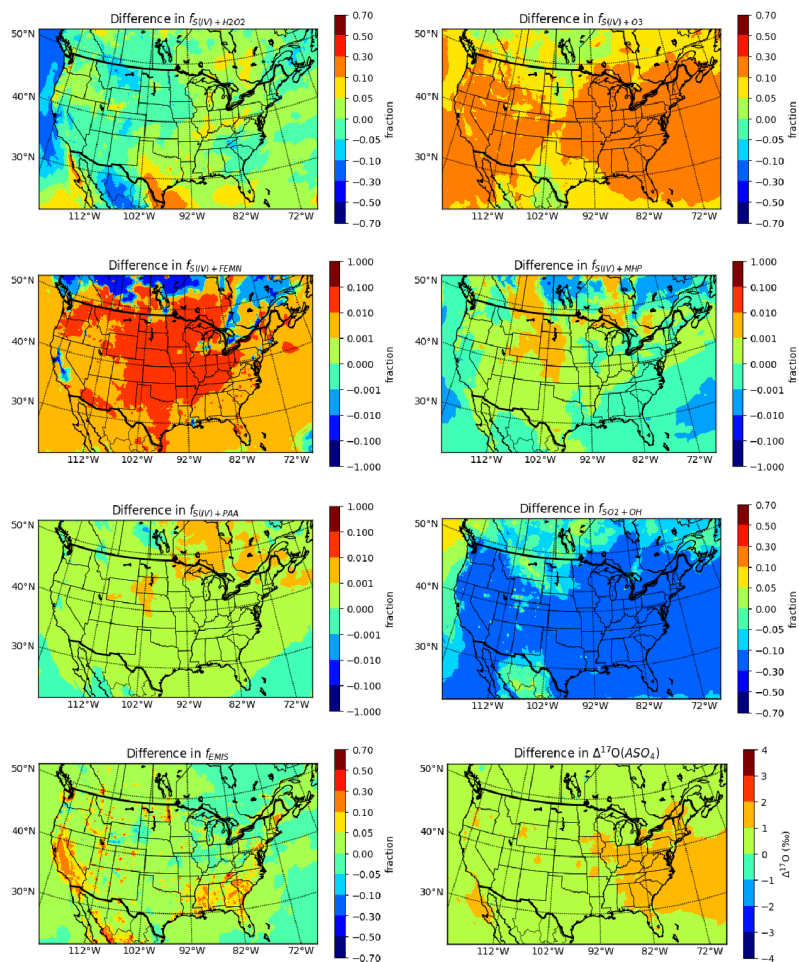
Fig. 7: The change in the fraction from each ASO₄ formation pathway and $\Delta^{17}O$ values across the contiguous US, from 2006 to 2019, based on CMAQ simulation.
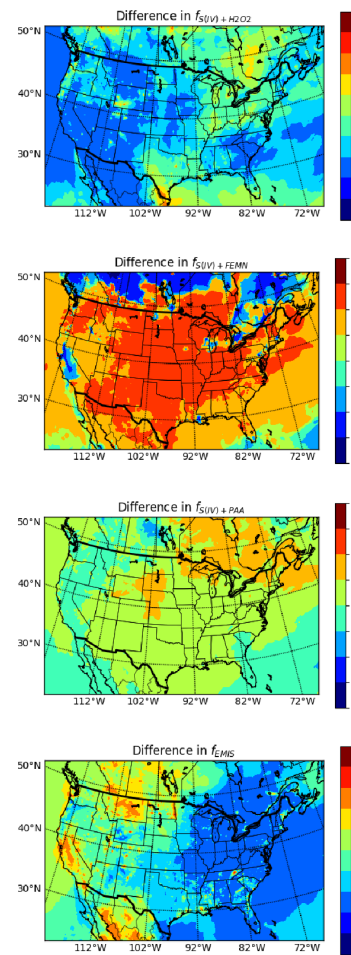
3.4 Comparison of Model $\Delta^{17}O(ASO_4)$ with Observations

The CMAQ simulations of $\Delta^{17}O(ASO_4)$ across the contiguous United States reveal significant insights into atmospheric ASO_4 formation over recent decades. However, observations of $\Delta^{17}O(ASO_4)$ in the contiguous US are very limited, with data primarily collected in the late 1990s at La Jolla, CA, and White Mountain Research Station, CA (Lee & Thiemens, 2001), and in the early 2000s at Baton Rouge, LA (Jenkins & Bao, 2006). These historical $\Delta^{17}O(ASO_4)$ data exhibit a range from 0.2‰ to 1.6‰ (Table S1). Due to the predicted change in ASO_4 chemistry from 2006 to 2019, the 2006 model simulation was chosen for evaluation against these observations (Fig. 8, 9). The comparison with historical $\Delta^{17}O(ASO_4)$ data is intended as a preliminary evaluation rather than a strict validation, given the temporal mismatch between the available observations (1990s–early 2000s) and the simulation years (2006, 2019). The observed range of 0.2‰ to 1.6‰ provides a useful benchmark for assessing whether the model produces realistic isotopic signatures. However, the limited number and dated nature of these measurements preclude a comprehensive validation of ASO_4 chemistry. This further emphasizes the critical need for new $\Delta^{17}O(ASO_4)$ observations within the contiguous United States to enable robust model-observation comparisons.

Generally, the CMAQ model reasonably reproduced $\Delta^{17}O(ASO_4)$ at the Baton Rouge, LA site, with a Root Mean Square Error (RMSE) of 0.20‰ ($n = 17$). This region is characterized by relatively low predicted $\Delta^{17}O(ASO_4)$ values, consistent with high regional SO_2 emissions and low cloud water pH that favor ASO_4 formation through aqueous $S(IV) + H_2O_2$ reactions. In contrast, the CMAQ-simulated $\Delta^{17}O(ASO_4)$ values tended to be overestimated at the California sites, suggesting possible inaccuracies in representing additional ASO_4 production pathways in this region. The La Jolla, CA site had an RMSE of 0.36‰ ($n=31$), while the White Mountain, CA site had a notably higher RMSE of 1.9‰ ($n=6$). Despite the limited number of $\Delta^{17}O(ASO_4)$ observations, a temporal analysis of model simulations versus observations indicates a consistent overprediction during the spring (Fig. 9). The $\Delta^{17}O(ASO_4)$ overestimation in spring could be associated with higher predicted cloud pH during this season, which promotes the $S(IV) + O_3$ oxidation pathway in the model (Fig. S26). The elevated cloud pH may result from increased NH_3 emissions, likely related to fertilizer use in surrounding agricultural areas or to underrepresentation of marine boundary layer processes that could influence ASO_4 production (Guo et al., 2017; Lim et al., 2022; Zheng et al., 2024; Wang et al., 2025). Given the strong nonlinear pH dependence of ASO_4 formation, even moderate NH_3 emission biases can produce significant changes in isotopic composition. Future work should include explicit sensitivity simulations to better quantify the coupled effects of NH_3, cloud pH, and oxidant chemistry on modeled $\Delta^{17}O(ASO_4)$. While organic acids (e.g., formic, acetic) can locally influence cloud water acidity, their contribution to bulk pH is generally minor relative to the dominant SO_2-H_2SO_4-NH_3 system (Herrmann et al., 2015; Shah et al., 2020; Tsui et al., 2019). Still, future model developments should evaluate their role in regional cloud pH and isotopic composition. Additionally, certain ASO_4 formation pathways, such as marine boundary layer chemistry involving $S(IV)$ oxidation by HOX, may not be fully captured, particularly at coastal sites like La Jolla, CA. These reactions can efficiently oxidize $S(IV)$ even under moderately acidic conditions and produce ASO_4 with relatively low $\Delta^{17}O$ signatures (Chen et al., 2016; Ishino et al., 2017), which may partly explain the model overestimation at this site. Another

possible factor is the omission of SO_2 oxidation via NO_2, an emerging multiphase pathway in polluted environments. Such reactions can proceed alongside metal-catalyzed and other aqueous pathways and are anticipated to result in low or near-zero $\Delta^{17}O$. Sensitivity simulations suggest that this mechanism can enhance ASO_4 concentrations by ~0.4-1.2% with a low rate constant and up to 4-20% with a higher rate constant, particularly under polluted, low-oxidant wintertime conditions, when the aqueous S(IV) oxidation by H_2O_2 and O_3 becomes less efficient (Sarwar et al., 2013), while its overall impact on $\Delta^{17}O(ASO_4)$ is expected to be minor.

Overall, the model-observation comparison of $\Delta^{17}O(ASO_4)$ suggests that CMAQ performs well in more acidic environments but struggles to simulate ASO_4 formation under less acidic conditions accurately. However, the limited availability of $\Delta^{17}O(ASO_4)$ observations constrains a more comprehensive evaluation of regional and temporal ASO_4 chemistry variations. This highlights the critical need for expanded observational datasets and model refinements to better represent the complex atmospheric ASO_4 dynamics. While this study highlights consistent patterns in ASO_4 oxidation pathways across the contiguous US, the evaluation of $\Delta^{17}O(ASO_4)$ remains constrained by the limited and dated nature of available measurements. Expanded and more recent datasets will be essential to validate and extend the findings presented here, particularly to quantify seasonal and regional variability in ASO_4 formation.
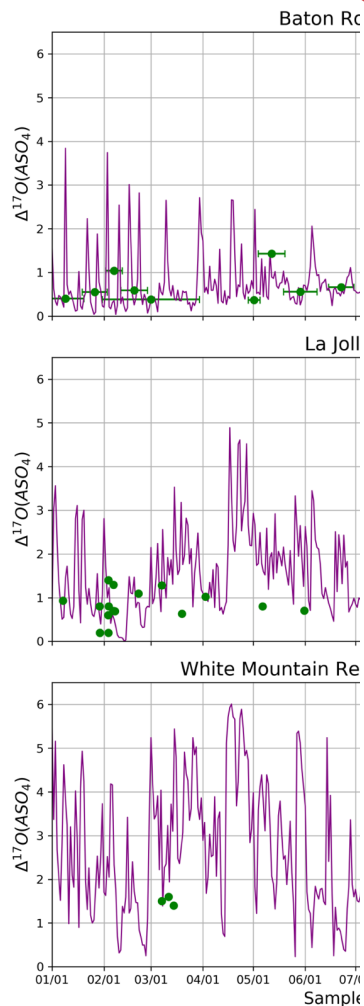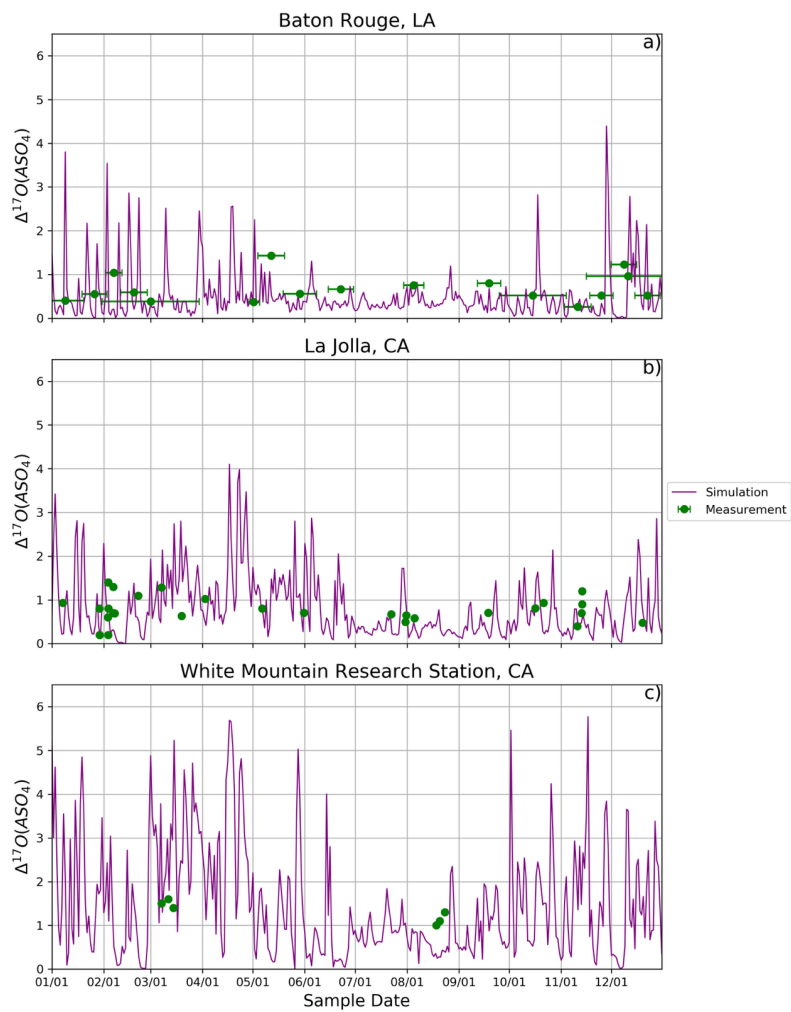
860   **Fig. 8: Temporal variations in $\Delta^{17}O(ASO_4)$ measurements and model simulations at a). Baton Rouge, LA (top); b) La Jolla, CA (middle); and c) White Mountain Research Station, CA (bottom). The x-axis error bars correspond to collection times.**

865
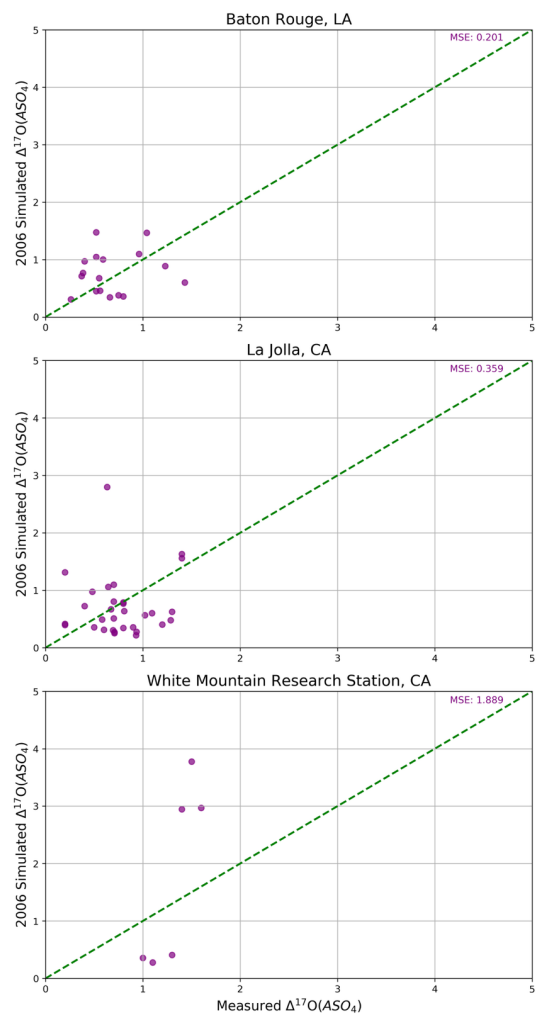
Fig. 9: Comparison of $\Delta^{17}O(ASO_4)$ measurements and model simulations at La Jolla, CA, White Mountain Research Station, CA, and Baton Rouge, LA from 1996 to 2005.
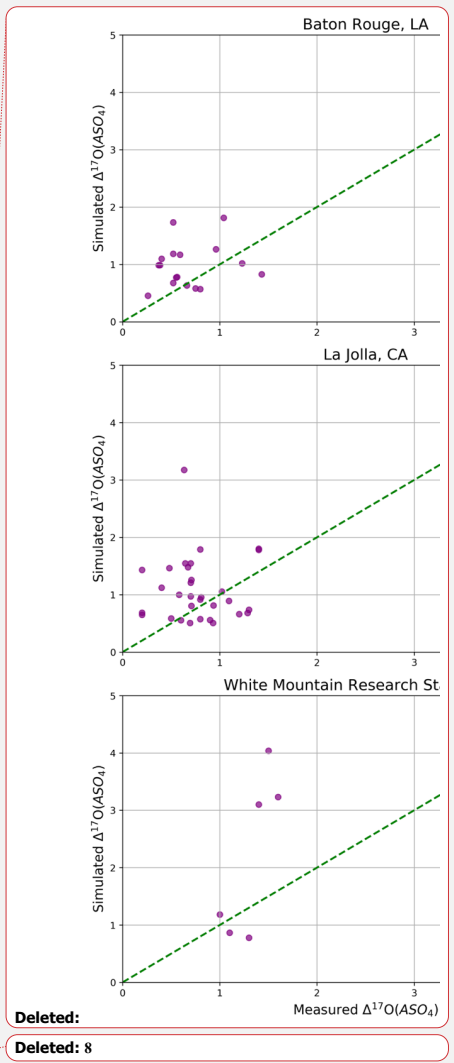
4 Conclusions

This study modeled ASO_4 formation pathways and the $\Delta^{17}O(ASO_4)$ for the contiguous United States using the CMAQ model for 2006 and 2019. The results reveal distinct seasonal and regional patterns in ASO_4 chemistry, strongly influenced by photochemical conditions, emissions of SO_2 and NH_3, and variations in cloud pH. From 2006 to 2019, significant changes in ASO_4 formation dynamics were observed, driven primarily by regulatory-driven reductions in SO_2 emissions. These shifts highlight the evolving balance between aqueous-phase oxidation pathways, particularly those driven by H_2O_2 and O_3.

The reductions in SO_2 emissions due to the Clean Air Act resulted in lower cloud water ASO_4, which subsequently increased cloud pH. This change shifted ASO_4 production toward the O_3 pathway, particularly in the eastern US, where the O_3 pathway was once limited by lower pH levels in 2006. By 2019, ASO_4 formation via O_3 oxidation had increased significantly, indicating a more efficient production mechanism under elevated pH conditions. The sub-linear response of ASO_4 concentrations to SO_2 emission reductions highlights the complexity of ASO_4 formation chemistry and the role of co-emitted species, such as NH_3, in modifying pH levels and influencing pathway dominance.

The isotopic signature $\Delta^{17}O(ASO_4)$ serves as a powerful tracer for tracking shifts in ASO_4 formation pathways. In regions with limited photochemical activity, such as during winter or in areas with high primary ASO_4 emissions, lower $\Delta^{17}O$ values were associated with greater contributions from primary ASO_4 emissions. Conversely, higher $\Delta^{17}O$ values reflected an increased role of the O_3 pathway, particularly in regions with elevated cloud pH, reduced SO_2 emissions, and higher ozone concentrations.

This work demonstrates a significant and predictable shift in ASO_4 chemistry over the study period. The introduction of $\Delta^{17}O(ASO_4)$ as a diagnostic tool for probing ASO_4 formation mechanisms provides a novel approach for investigating these changes. Expanding the measurement of $\Delta^{17}O(ASO_4)$ across diverse regions and time periods will be critical for validating and extending these findings. Future studies should prioritize exploring how changes in atmospheric composition and regulatory measures continue to influence ASO_4 chemistry, with a particular focus on understanding the increasing prominence of O_3-driven chemistry. This effort will be crucial for enhancing atmospheric models and understanding the implications of ASO_4 chemistry on air quality, human health, and climate.

Code and Data Availability: The source code for CMAQ version 5.4 is available at https://github.com/USEPA/CMAQ/tree/5.4 (last access: 1 March 2025). The input datasets for CMAQ simulation are available

at https://cmas-equates.s3.amazonaws.com/index.html#CMAQ_12US1/INPUT/ (last access: 1 March 2025). The in-detail simulation results for $\Delta^{17}O(ASO_4)$ are achieved on Zenodo.org (https://doi.org/10.5281/zenodo.14954960, Fang, 2025).

Author contributions: HF and WWW designed the study. HF conducted the model simulations and analysis with input from WWW. HF wrote the manuscript with input from all authors. WWW secured funding.

Competing Interests: The contact author has declared that none of the authors have competing interests.

Acknowledgements: We thank Kristen Foley for providing the base model input files. We thank Myk Milligan and Nathan Elger and the staff of the Hyperion cluster for helping to install CMAQ, transferring data, and maintaining the computing cluster

Financial Support: This research has been supported by NSF AGS (2414561 and 2441725), NSF EPSCOR RII Track-4 (2410015), and USC start-up funds.

References

Alexander, B., Park, R. J., Jacob, D. J., & Gong, S.: Transition metal-catalyzed oxidation of atmospheric sulfur: Global implications for the sulfur budget. Journal of Geophysical Research: Atmospheres, 114(D2), doi:10.1029/2008JD010486, 2009.

Alexander, B., Park, R. J., Jacob, D. J., Li, Q. B., Yantosca, R. M., Savarino, J., Lee, C. C. W., & Thiemens, M. H.: Sulfate formation in sea-salt aerosols: Constraints from oxygen isotopes. Journal of Geophysical Research, 110, D10307, doi:10.1029/2004JD005659, 2005.

Alexander, B., Savarino, J., Kreutz, K. J., & Thiemens, M. H.: Impact of preindustrial biomass-burning emissions on the oxidation pathways of tropospheric sulfur and nitrogen. Journal of Geophysical Research, 109, D08303, doi:10.1029/2003JD004218, 2004.

Appel, K. W., Bash, J. O., Fahey, K. M., Foley, K. M., Gilliam, R. C., Hogrefe, C., ... & Wong, D. C.: The Community Multiscale Air Quality (CMAQ) model versions 5.3 and 5.3. 1: system updates and evaluation. Geoscientific Model Development, 14(5), 2867-2897, doi:10.5194/gmd-14-2867-2021, 2021.

Arimoto, R., Nottingham, A. S., Webb, J., Schloesslin, C. A., & Davis, D. D.: Non-sea salt sulfate and other aerosol constituents at the South Pole during ISCAT. Geophysical Research Letters, 28(19), 36453648, doi:10.1029/2000GL012714, 2001.

Barkan, E., & Luz, B.: High-precision measurements of $^{17}O/^{16}O$ and $^{18}O/^{16}O$ of O_2 and O_2/Ar ratio in air. Rapid Communications in Mass Spectrometry, 17(24), 28092814, doi:10.1002/rcm.1267, 2003.

Benish, S. E., Bash, J. O., Foley, K. M., Appel, K. W., Hogrefe, C., Gilliam, R., & Pouliot, G.: Long-term regional trends of nitrogen and sulfur deposition in the United States from 2002 to 2017. Atmospheric Chemistry and Physics, 22(19), 12749-12767, doi:10.5194/acp-22-12749-2022, 2022.

Bhattacharya, S. K., Pandey, A., & Savarino, J.: Determination of intramolecular isotope distribution of ozone by oxidation reaction with silver metal. Journal of Geophysical Research: Atmospheres, 113(D3), doi:10.1029/2006JD008309, 2008.

Bianchi, F., Kurtén, T., Riva, M., Mohr, C., Rissanen, M. P., Roldin, P., ... & Ehn, M.: Highly oxygenated organic molecules (HOM) from gas-phase autoxidation involving peroxy radicals: A key contributor to atmospheric aerosol. Chemical reviews, 119(6), 3472-3509, doi:10.1021/acs.chemrev.8b00395, 2019.

Calvo, A. I., Alves, C., Castro, A., Pont, V., Vicente, A. M., & Fraile, R.: Research on aerosol sources and chemical composition: Past, current and emerging issues. Atmospheric Research, 120, 1-28, doi:10.1016/j.atmosres.2012.09.021, 2013.

Chen, Q., Geng, L., Schmidt, J. A., Xie, Z., Kang, H., Dachs, J., ... & Alexander, B.: Isotopic constraints on the role of hypohalous acids in sulfate aerosol formation in the remote marine boundary layer. Atmospheric Chemistry and Physics, 16(17), 11433-11450, doi:10.5194/acp-16-11433-2016, 2016.

Dominguez, G., Jackson, T., Brothers, L., Barnett, B., Nguyen, B., & Thiemens, M. H.: Discovery and measurement of an
isotopically distinct source of sulfate in Earth's atmosphere. Proceedings of the National Academy of Sciences, 105(35),
12,769 12,773, doi:10.1073/pnas.0805255105, 2008.

Fahey, K. M., & Pandis, S. N.: Optimizing model performance: variable size resolution in cloud chemistry modeling.
Atmospheric Environment, 35(26), 4471-4478, 2001.

Fang, H.: Simulating $\Delta^{17}O$ of sulfate aerosol within the contiguous United States to trace the formation processes, Zenodo
[data set], doi:10.5281/zenodo.14954960, 2025.

Foley, K. M., Pouliot, G. A., Eyth, A., Aldridge, M. F., Allen, C., Appel, K. W., ... & Adams, E.: 2002-2017 anthropogenic
emissions data for air quality modeling over the United States. Data in Brief, 47, 109022, doi:10.1016/j.dib.2023.109022, 2023

Guo, H., Weber, R. J., & Nenes, A.: High levels of ammonia do not raise fine particle pH sufficiently to yield nitrogen oxide-
dominated sulfate production. Scientific Reports, 7(1), 12109, 2017.

Hallquist, M., Wenger, J. C., Baltensperger, U., Rudich, Y., Simpson, D., Claeys, M., ... & Wildt, J.: The formation, properties
and impact of secondary organic aerosol: current and emerging issues. Atmospheric chemistry and physics, 9(14), 5155-5236,
doi:10.5194/acp-9-5155-2009, 2009.

Harris, E., Sinha, B., Van Pinxteren, D., Tilgner, A., Fomba, K. W., Schneider, J., ... & Herrmann, H.: Enhanced role of
transition metal ion catalysis during in-cloud oxidation of SO_2. science, 340(6133), 727-730, doi:10.1126/science.1230911,
2013

Hattori, S., Iizuka, Y., Alexander, B., Ishino, S., Fujita, K., Zhai, S., ... & Yoshida, N.: Isotopic evidence for acidity-driven
enhancement of sulfate formation after SO2 emission control. Science Advances, 7(19), eabd4610, 2021.

Haywood, J., & Boucher, O. (2000). Estimates of the direct and indirect radiative forcing due to tropospheric aerosols: A re.
Res of Geophysics, 38(4), 513 543, doi:10.1029/1999RG000078, 2000.

Herrmann, H., Schaefer, T., Tilgner, A., Styler, S. A., Weller, C., Teich, M., & Otto, T.: Tropospheric aqueous-phase
chemistry: kinetics, mechanisms, and its coupling to a changing gas phase. Chemical reviews, 115(10), 4259-4334, 2015.

Ishino, S., Hattori, S., Savarino, J., Jourdain, B., Preunkert, S., Legrand, M., et al.: Seasonal variations of triple oxygen isotopic
compositions of atmospheric sulfate, nitrate, and ozone at Dumont d'Urville, coastal Antarctica. Atmospheric Chemistry and
Physics, 17(5), 3713 3727, doi:10.5194/acp 17 3713 2017, 2017.

Itahashi, S., Hattori, S., Ito, A., Sadanaga, Y., Yoshida, N., & Matsuki, A.: Role of dust and iron solubility in sulfate formation
during the long-range transport in East Asia evidenced by 17O-excess signatures. Environmental Science & Technology,
56(19), 13634-13643, 2022.

Jenkins, K. A., & Bao, H.: Multiple oxygen and sulfur isotope compositions of atmospheric sulfate in Baton Rouge, LA, USA.
Atmospheric Environment, 40(24), 4528-4537, doi:10.1016/j.atmosenv.2006.04.010, 2006.

Jones, A. D. L. A., Roberts, D. L., & Slingo, A.: A climate model study of indirect radiative forcing by anthropogenic sulphate
aerosols. Nature, 370(6489), 450-453, doi:10.1038/370450a0, 1994.

Kaiser, J., Röckmann, T., & Brenninkmeijer, C. A.: Contribution of mass-dependent fractionation to the oxygen isotope anomaly of atmospheric nitrous oxide. Journal of Geophysical Research, 109, D033055, doi:10.1029/2003JD004088, 2004.

Kaufman, Y. J., & Tanré, D.: Effect of variations in super-saturation on the formation of cloud condensation nuclei. Nature, 369(6475), 45-48, doi:10.1038/369045a0, 1994.

Langner, J., Rodhe, H., Crutzen, P. J., & Zimmermann, P.: Anthropogenic influence on the distribution of tropospheric sulphate aerosol. Nature, 359(6397), 712-716, doi:10.1038/359712a0, 1992.

Lee, C. C. W., & Thiemens, M. H.: The $\delta^{17}O$ and $\delta^{18}O$ measurements of atmospheric sulfate from a coastal and high alpine region: A mass independent isotopic anomaly. Journal of Geophysical Research: Atmospheres, 106(D15), 17359-17373, doi:10.1029/2000JD900805, 2001.

Li, J., Zhang, Y. L., Cao, F., Zhang, W., Fan, M., Lee, X., & Michalski, G.: Stable sulfur isotopes revealed a major role of transition-metal ion-catalyzed SO2 oxidation in haze episodes. Environmental Science & Technology, 54(5), 2626-2634, doi:10.1021/acs.est.9b07150, 2020.

Liang, J., & Jacobson, M. Z.: A study of sulfur dioxide oxidation pathways over a range of liquid water contents, pH values, and temperatures. Journal of Geophysical Research, 104(D11), 13,74913,769, doi:10.1029/1999JD900097, 1999.

Lim, J., Park, H., & Cho, S.: Evaluation of the ammonia emission sensitivity of secondary inorganic aerosol concentrations measured by the national reference method. Atmospheric Environment, 270, 118903, 2022.

Lin, Y. C., Zhao, Y., Zhang, Y. L., Hong, Y., Hattori, S., Itahashi, S., ... & Thiemens, M. H.: China's SO2 emission reductions enhance atmospheric ozone–driven sulfate aerosol production in East Asia. Proceedings of the National Academy of Sciences, 122(24), e2414064122, 2025.

Liu, L., Bei, N., Wu, J., Liu, S., Zhou, J., Li, X., ... & Li, G.: Effects of stabilized Criegee intermediates (sCIs) on sulfate formation: a sensitivity analysis during summertime in Beijing–Tianjin–Hebei (BTH), China. Atmospheric Chemistry and Physics, 19(21), 13341-13354, doi:10.5194/acp-19-13341-2019, 2019.

Lohmann, U., & Feichter, J.: Impact of sulfate aerosols on albedo and lifetime of clouds: A sensitivity study with the ECHAM4 GCM. Journal of Geophysical Research: Atmospheres, 102(D12), 13685-13700, doi:10.1029/97JD00631, 1997.

Meidan, D., Holloway, J. S., Edwards, P. M., Dube, W. P., Middlebrook, A. M., Liao, J., ... & Rudich, Y.: Role of Criegee intermediates in secondary sulfate aerosol formation in nocturnal power plant plumes in the Southeast US. ACS Earth and Space Chemistry, 3(5), 748-759, doi:10.1021/acsearthspacechem.8b00215, 2019.

Michalski, G. M., Scott, Z., Kabiling, M., and Thiemens, M. H.: First measurements and modeling of ^{17}O in atmospheric nitrate, Geophys. Res. Lett., 30, 1870, doi:10.1029/2003GL017015, 2003.

Morin, S., Savarino, J., Bekki, S., Gong, S., & Bottenheim, J. W.: Signature of Arctic surface ozone depletion events in the isotope anomaly (17O) of atmospheric nitrate. Atmospheric Chemistry and Physics, 7(5), 14511469, doi:10.5194/acp-7-1451-2007, 2007.

Pandis, S. N., & Seinfeld, J. H.: Sensitivity analysis of a chemical mechanism for aqueous-phase atmospheric chemistry. Journal of Geophysical Research, 94(D1), 11051126, doi:10.1029/JD094iD01p01105, 1989.

Peng, Y., Hattori, S., Zuo, P., Ma, H., & Bao, H.: Record of pre-industrial atmospheric sulfate in continental interiors. Nature Geoscience, 16(7), 619-624, 2023.

Pye, H. O., Nenes, A., Alexander, B., Ault, A. P., Barth, M. C., Clegg, S. L., ... & Zuend, A.: The acidity of atmospheric particles and clouds. Atmospheric chemistry and physics, 20(8), 4809-4888, 2020.

Reiss, R., Anderson, E. L., Cross, C. E., Hidy, G., Hoel, D., McClellan, R., & Moolgavkar, S.: Evidence of health impacts of sulfate-and nitrate-containing particles in ambient air. Inhalation toxicology, 19(5), 419-449, doi:10.1080/08958370601174941, 2007.

Sarwar, G., Fahey, K., Kwok, R., Gilliam, R. C., Roselle, S. J., Mathur, R., ... & Carter, W. P.: Potential impacts of two SO2 oxidation pathways on regional sulfate concentrations: Aqueous-phase oxidation by NO2 and gas-phase oxidation by Stabilized Criegee Intermediates. Atmospheric Environment, 68, 186-197, 2013.

Savarino, J., Bekki, S., ColeDai, J., & Thiemens, M. H.: Evidence from sulfate mass independent oxygen isotopic compositions of dramatic changes in atmospheric oxidation following massive volcanic eruptions. Journal of Geophysical Research, 108(D21), 4671, doi:10.1029/2003JD003737, 2003.

Savarino, J., Kaiser, J., Morin, S., Sigman, D. M., & Thiemens, M. H.: Nitrogen and oxygen isotopic constraints on the origin of atmospheric nitrate in coastal Antarctica. Atmospheric Chemistry and Physics, 7(8), 19251945, doi:10.5194/acp-7-1925-2007, 2007.

Savarino, J., Lee, C. C., & Thiemens, M. H.: Laboratory oxygen isotopic study of sulfur (IV) oxidation: Origin of the mass-independent oxygen isotopic anomaly in atmospheric sulfates and sulfate mineral deposits on Earth. Journal of Geophysical Research, 105(D23), 29,07929,088, doi:10.1029/2000JD900456, 2000.

Seigneur, C., & Saxena, P.: A theoretical investigation of sulfate formation in clouds. Atmospheric Environment (1967), 22(1), 101-115, doi:10.1016/0004-6981(88)90303-4, 1988.

Shah, V., Jacob, D. J., Moch, J. M., Wang, X., & Zhai, S.: Global modeling of cloud water acidity, precipitation acidity, and acid inputs to ecosystems. Atmospheric Chemistry and Physics, 20(20), 12223-12245, 2020.

Smith, S. J., van Aardenne, J., Klimont, Z., Andres, R. J., Volke, A., & Delgado Arias, S.: Anthropogenic sulfur dioxide emissions: 18502005. Atmospheric Chemistry and Physics, 11(3), 1101-1116, doi:10.5194/acp-11-1101-2011, 2011.

Sofen, E. D., Alexander, B., & Kunasek, S. A.: The impact of anthropogenic emissions on atmospheric sulfate production pathways, oxidants, and ice core $\Delta^{17}O(SO_4^{2-})$. Atmospheric Chemistry and Physics, 11(7), 3565-3578, doi:10.5194/acp-11-3565-2011, 2011.

Tsui, W. G., Woo, J. L., & McNeill, V. F.: Impact of aerosol-cloud cycling on aqueous secondary organic aerosol formation. Atmosphere, 10(11), 666, 2019.

U.S. Environmental Protection Agency: CMAQ release notes: Process analysis & sulfur tracking model (STM). In USEPA/CMAQ Wiki. GitHub. https://github.com/USEPA/CMAQ/wiki/CMAQ-Release-Notes:-Process-Analysis-&-Sulfur-Tracking-Model-(STM), last access: 9 October 2025.

Vannucci, P. F., Foley, K., Murphy, B. N., Hogrefe, C., Cohen, R. C., & Pye, H. O.: Temperature-Dependent Composition of
Summertime PM2. 5 in Observations and Model Predictions across the Eastern US. ACS Earth and Space Chemistry, 8(2),
381-392, doi:10.1021/acsearthspacechem.3c00333, 2024.

Vicars, W. C., & Savarino, J.: Quantitative constraints on the O-17-excess (Delta 17O) signature of surface ozone: Ambient
measurements from 50 N to 50 S using the nitrite-coated filter technique. Geochimica et Cosmochimica Acta, 135, 270-287,
doi:10.1016/j.gca.2014.03.023, 2014.

Wang, X., Tsimpidi, A. P., Luo, Z., Steil, B., Pozzer, A., Lelieveld, J., & Karydis, V. A.: The influence of ammonia emission
inventories on size-resolved global atmospheric aerosol composition and acidity. Atmospheric Chemistry and Physics, 25(18),
10559-10586, 2025.

Walcek, C. J., & Taylor, G. R.: A theoretical method for computing vertical distributions of acidity and sulfate production
within cumulus clouds. Journal of Atmospheric Sciences, 43(4), 339-355, 1986.

Walters, W. W., Michalski, G., Böhlke, J. K., Alexander, B., Savarino, J., & Thiemens, M. H.: Assessing the seasonal dynamics
of nitrate and sulfate aerosols at the South Pole utilizing stable isotopes. Journal of Geophysical Research: Atmospheres,
124(14), 8161-8177. doi:10.1029/2019JD030517, 2019.

Weber, R. J., Guo, H., Russell, A. G., & Nenes, A.: High aerosol acidity despite declining atmospheric sulfate concentrations
over the past 15 years. Nature Geoscience, 9(4), 282-285, doi:10.1038/ngeo2665, 2016.

Weston, R. E. Jr.: When is an isotope effect non-mass dependent. Journal of Nuclear Science and Technology, 43(4), 295299,
doi:10.1080/18811248.2006.9711092, 2006.

Yarwood, G., Jung, J., Whitten, G. Z., Heo, G., Mellberg, J., & Estes, M.: Updates to the Carbon Bond mechanism for version
6 (CB6), in : Proceedings the of 9th Annual CMAS Conference, Chapel Hill, NC, October 11-13, 2010, 11-13, 2010.

Zheng, G., Su, H., Andreae, M. O., Pöschl, U., & Cheng, Y.: Multiphase buffering by ammonia sustains sulfate production in
atmospheric aerosols. AGU Advances, 5(4), e2024AV001238, 2024.

Page 4: [1] Deleted	Fang, Huan	10/10/25 12:49:00 AM

Page 4: [2] Deleted	Fang, Huan	10/10/25 12:49:00 AM

Page 4: [3] Deleted	Fang, Huan	10/10/25 12:49:00 AM

Page 11: [4] Deleted	Fang, Huan	10/10/25 12:49:00 AM

Page 11: [4] Deleted	Fang, Huan	10/10/25 12:49:00 AM

Page 11: [4] Deleted	Fang, Huan	10/10/25 12:49:00 AM

Page 11: [4] Deleted	Fang, Huan	10/10/25 12:49:00 AM